

# Design and performance characteristics of solar adsorption refrigeration system using parabolic trough collector: Experimental and statistical optimization technique



Nidal H. Abu-Hamdeh<sup>\*</sup>, Khaled A. Alnefaie<sup>1</sup>, Khalid H. Almitani<sup>2</sup>

Mechanical Engineering Department, Faculty of Engineering, King Abdulaziz University, P.O. Box 80204, Jeddah 21589, Saudi Arabia

## ARTICLE INFO

### Article history:

Received 3 January 2013

Accepted 24 April 2013

Available online 5 June 2013

### Keywords:

Solar adsorption

Parabolic trough solar collector

Adsorbent

Adsorbate

Coefficient of performance

## ABSTRACT

The current work demonstrates a developed model of a solar adsorption refrigeration system with specific requirements and specifications. The recent scheme can be employed as a refrigerator and cooler unit suitable for remote areas. The unit runs through a parabolic trough solar collector (PTC) and uses olive waste as adsorbent with methanol as adsorbate. Cooling production,  $COP$  (coefficient of performance), and  $COP_a$  (cycle gross coefficient of performance) were used to assess the system performance. The system's design optimum parameters in this study were arrived to through statistical and experimental methods. The lowest temperature attained in the refrigerated space was 4 °C and the equivalent ambient temperature was 27 °C. The temperature started to decrease steadily at 20:30 – when the actual cooling started – until it reached 4 °C at 01:30 in the next day when it rose again. The highest  $COP_a$  obtained was 0.75.

© 2013 Elsevier Ltd. All rights reserved.

## 1. Introduction

Cooling devices work on solar adsorption are of excessive demand to reach the need for refrigeration demands such as food preservation, air-conditioning, and medicative/nutrient conservation in remote areas [1]. Additionally, these devices are quiet, non-destructive and biodegradable. The application of insolation perceives widespread consideration as a consequence of the globe energy deficiency. Cooling in specifically is desirable as an application of solar-energy due to the occurrence of highest loads of cooling with the existing solar power. Coolers powered by the sun possess means to elevate the life denomination of populations residing in locations which are electricity insufficient. Solar cooling for cold storage of food mounts up latent heat, hence directing to lesser volume of refrigerators [2]. Hassan and Mohamad [3] presented a thorough review of literature on adsorption based air conditioning and cooling devices that are operated by solar power. They reported the different systems alongside with their thermodynamic working principles. Gonzalez and Rodriguez [4] investigated the usage of solar adsorption refrigeration for food and vaccine storage. Hassan et al. [5] investigated the effect of several

adsorption technique factors on its execution. They performed a parametric study on their proposed adsorption refrigeration device that could yield chill continuously during the day. Hassan and Mohamad [6] in their study on preceding investigators and improvements of the solar powered closed physisorption cooling devices reported numerical and experimental simulation studies as well as means that are proposed to increase the process performance. Despite their advantages, the adsorption refrigeration units have deficiencies like low  $COP$ , high weight and elevated cost. Choudhury et al. [7] explained the main reason behind the unsuccessful commercialization of the adsorption cooling systems. They said that it is because of their low specific cooling power, relatively bigger sizes of adsorption based cooling units are required. They stated “Recent application of nano-technology in the development of adsorbent material may be a big step forward towards making this technology competitive with available technologies in the market”. Different procedures have been performed to surpass inconveniences of adsorption refrigeration units. Some of these approaches include enhancement of mass and heat transfer in the adsorber, improvement on the dissipation traits of the adsorbent/adsorbate pairs, study and fabricate of various types of systems and enhancement of regenerative mass and heat transfer among beds [8]. Habib et al. [9] showed that even when low-temperature heat source exists the mutual adsorption cycles are possible. Theoretical modeling of a solar adsorption cooling device that uses activated carbon-methanol was performed by [10]. Their modeling represented the transfer of mass and heat within all components of the adsorption system. Upon solving their model, they obtained a

<sup>\*</sup> Corresponding author. Tel.: +966 2 6402000x68256; mobile: +966 545993930; fax: +966 2 6952181.

E-mail addresses: [nidal@just.edu.jo](mailto:nidal@just.edu.jo) (N.H. Abu-Hamdeh), [kalnefaie@kau.edu.sa](mailto:kalnefaie@kau.edu.sa) (K.A. Alnefaie), [khalidalmitani@gmail.com](mailto:khalidalmitani@gmail.com) (K.H. Almitani).

<sup>1</sup> Tel.: +966 2 6952277; mobile: +966 553000305; fax: +966 2 6952181.

<sup>2</sup> Tel.: +966 2 6952277; mobile: +966 594202180; fax: +966 2 6952181.

specific cooling power and COP of the device as 0.211 and 2.326, respectively. Furthermore, they found that the distribution of pressure was almost uniform within the bed and changing with time only.

Being cost-effective, friendly to the environment, and with low requirement of maintenance makes the adsorption systems among the solar thermal refrigeration methods that own capability in the close future. Nonetheless, economical and technical constraints are the main factors that limit the broad application of these systems. To rise above these problems escalating research actions in this area exist. A majority of the analysis administered on these systems has been attained with either evacuated tube or flat plate collectors, whereas less attention has been given to the parabolic trough collectors (PTCs). The PTC is among the family of solar collectors currently receiving considerable attention. They are used for a number of different uses, including hot-water and industrial steam production [11–15]. When compared parabolic trough collector to flat plate collectors, Valan Arasu and Sornakumar [16] mentioned that the large amount of adsorption that could be obtained with PTC offsets the drawback linked with the necessity of certain level of tracking. Furthermore, parabolic trough collectors are structurally simpler than other collectors. Badran and Eck [17] stated that PTCs are the most organized and advanced type of solar collectors, and they have high efficiency. As stated by Valan Arasu and Sornakumar [18], PTCs technology is considered the most established-solar technology in fabrication and operational testing.

Another important element of the solar adsorption cooling unit that requires going over is the adsorber. During latest years, many solar adsorption cooling units were examined with various collections of adsorbents and adsorbates. Anyanwu [19] presented a review of the main concepts and ideas of solid adsorption solar refrigeration. He reported about the main principles for the selection process of suitable adsorbent/adsorbent pairs. In addition, adsorption balance patterns that justify the adsorption properties of a pair of adsorbent/adsorbate and operate as reference equations in analytical models of the system were reported. The literature reveals that the most considered pairs in this domain are zeolite/water, activated carbon/methanol, activated carbon/ammonia, and silica gel/water. An ideal pair of adsorbate–adsorbent cannot be found, and hence, when an alternative is decided it has to be an adjustment that holds most of the required characteristics as possible. Anyanwu and Ezekwe [20] utilized activated carbon/methanol as the adsorbent/adsorbate pair in their solid adsorption solar refrigerator. They found that only 2% of the incident solar radiation was transformed into cooling effect in the tropical climate of Nigeria. [21] presented a predictive model for a solar powered ice maker which used activated carbon–methanol pair in a hot and humid location. They used a static solar collector that was covered by translucent insulation material paired to an adsorptive bed. After six months from the beginning of measurements they obtained a net COP of 0.13. Silica gel–water as an adsorbent/adsorbate pair had been used in several studies [22–24]. For example, Wang et al. [23] developed a novel silica gel–water adsorber. In order to increase the adsorber performance when it is operated by a low temperature heat supply, just one vacuum valve was installed between the two adsorption/desorption vacuum chambers. Their test results confirmed that the operational dependability of the chiller was greatly improved because of less moving elements in their unit. Critoph and Vogel [25] found refrigerant R22 to work best with activated carbon out of organic refrigerants measured. Karaca et al. [26] determined adsorption isotherms of methylene blue for pyrolysed and raw coal samples. According to their results, the maximum adsorption capacity was found with the raw coal sample while adsorption capacity declined with rising pyrolysis temperature. El-Sharkawy et al. [27] studied the operation of

adsorption cooling system using activated charcoal/methanol and Maxsorb III/methanol pairs. Their computations showed the dominance of Maxsorb III/methanol pair for both of ice-making and air-conditioning applications. [28] presented a thermodynamic framework to capture the relationship between the specific surface area ( $A_i$ ) and the energy factor. They proposed theoretical framework of specific surface area ( $A_i$ ) and heat of adsorption ( $\Delta H^\circ$ ) that provides valuable guides for researchers in developing advanced porous adsorbents for methane and hydrogen uptake. This is the basis for which activated charcoal from olive waste as adsorbent was researched. Olive waste (sometimes called “olive cake” or “jift”) are the solid remainders acquired by crushing olives; they are of the most excessive agricultural related litters in the area of the Mediterranean Sea creating many problems by their accession and disposal [29]. The olive cake is presently used as an amendment and fertilizer, as an added ingredient to fodder and as a supply of heat energy [29]. Alteration of this “jift” into a useful adsorbent contributes to minimize the solid wastes and using a resource that otherwise went into a waste.

This research article exhibits the analysis of a solar adsorption cooling system with particular requirements and specifications to be utilized as a cooling and an air conditioning unit appropriate to be operated in remote areas. A preliminary first prototype system that originates and develops a thermally driven sorption technology as an alternative to compressor refrigeration devices was presented in Abu-Hamdeh and Al-Muhtaseb [2]. For the advancement of the general system performance and productivity, the current study uses PTC instead of flat plate collector with the purpose of improving its overall performance and productivity. A statistical study is administered to assess some optimal operating and design parameters of the system.

## 2. Description of the prototype

An illustrative representation of the concentration cooling system is illustrated in Fig. 1. It consists of a solar concentrator (PTC), heat storage tank, adsorber's bed, condenser, evaporator, throttling valve, and circulating pump. To attain the highest yearly energy harvest, the single-axis tracking collector is aligned on a south–north line and tracking the sun from east to west. The parameters that characterized the PTC module are listed in Table 1. The receiver is a stainless steel tube positioned along the focal line of the concentrator. In order to reduce convection and radiation heat losses the tube is covered by a glass envelope. The adsorbent bed ( $1.80 \times 0.80 \times 0.2$  m thick) is made of steel casings tilted  $40^\circ$  from the ground. There were four bed steel tubes; each has an outer and inner diameter of 70.2 and 64.3 mm, respectively. Each tube has a length 1800 mm and a perforated coaxial inner tube of 20.1 and 15.9 mm outer and inner diameters, respectively. The holes' diameter was 2 mm, spaced 40 mm axially and five per perimeter in an irregular mode. Each gap between the outer and inner tube was filled with 1.5 kg of olive waste. After that, the pipes were adhered to the plate at a 100 mm pitch. The pipes from each end are connected to top and bottom headers. The headers are steel tubes with 27.6 and 21.8 mm outer and inner diameters, respectively. A dark sheet covers the bed and is put exactly above the tubes. The dark color increases the solar radiation absorption. A glass panel (5 mm thick) covers the bed and prevents the escape of the long-wave radiation and works the same as a greenhouse. A storage tank was used to store hot water coming from the receiver. A pump is used to circulate hot water from the storage tank through the bed and back to the storage tank. Steel tubes pass through the bed convey the hot water between top and bottom headers. Hot water passes through the bed is used to warm the adsorber and desorption of methanol from the adsorbent takes place.

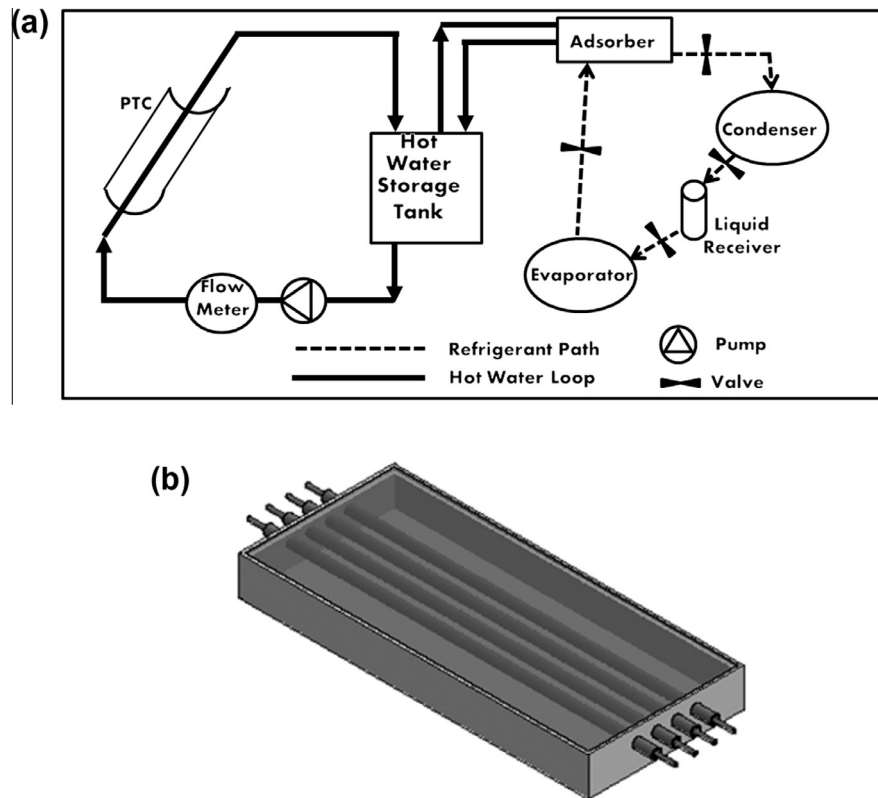


Fig. 1. (a) Schematic diagram of the parabolic trough solar collector (PTC) adsorption refrigeration system and (b) adsorber drawing.

**Table 1**  
Characteristics of the PTC Collector.

| Item                                    | Value              |
|---|--------------------|
| Collector aperture area                 | 3.7 m <sup>2</sup> |
| Collector aperture                      | 1.26 m             |
| Aperture-to-length ratio                | 0.58               |
| Rim angle                               | 90°                |
| Inner diameter of the absorber          | 35.5 mm            |
| Outer diameter of the absorber          | 40 mm              |
| Concentration ratio                     | 31.2               |
| Optical efficiency of the collector (%) | 76.5               |
| Parabolic rib thickness                 | 20 mm              |

A condenser is a heat conversion device in which desorbed refrigerant (methanol) drifts through one or several pipes. The desorbed vapor refrigerant flows from the bed tubes into the condenser via control valve to be changed into liquid refrigerant. In this system, the condenser is a simple steel tube of 1.90 m length, 12.23 mm outer diameter, and 9.87 mm inner diameter. The condensed liquid methanol flows by gravity into a liquid receiver via a flow control valve. The liquid receiver is a vertical cylinder made-up of galvanized steel sheet that has a 120 mm diameter and 300 mm length. The liquid methanol flows from the receiver by gravity into an evaporator via a flow control valve. The evaporator is a device that interchanges heat between the liquid methanol drifted into it and the refrigerated space. The evaporator in this system consists of a spirally coiled copper tube of 11.6 mm outer diameter, 0.8 mm inner diameter and 110 mm total length that passes through a small refrigerator (refrigerated space). As a result of heat transfer from refrigerated space to the methanol in the evaporator, the methanol evaporates and flows via control valve to the bed to be adsorbed into the adsorbent. Hence, a *cooling effect* is created in the refrigerated space. The refrigerated space is used as a cold storage of food products operated at the night cycle.

Five thermocouples of Type T (copper-constantan) thermocouples, which are usually utilized for measuring temperatures between  $-150^{\circ}\text{C}$  and  $+350^{\circ}\text{C}$  with an accuracy of  $\pm 0.1^{\circ}\text{C}$ , were used to measure temperatures. Multichannel Recorder was used to register the temperatures. The temperatures measured were; bed temperature, condenser temperature, tube surface temperature, ambient temperature, and refrigerated space temperature. Masoneillan vacuum pressure gauges with a reading accuracy of  $\pm 0.1$  kPa were used to measure gauge pressures of range from  $-100$  to  $+200$  kPa. Eppley pyranometer was used to measure the total solar radiation incident on the bed surface. The device was mounted in the same plane as the adsorbent bed. A digital counter connected to the pyranometer with a reading accuracy within 5% of the actual values was used to read the cumulative incident energy at intervals of 30 min.

### 3. Experimental method and adsorbent preparation

#### 3.1. Preparation of the adsorbent

Olive waste is a result of olive oil production. In order to get rid of the remaining oil, hexane was used to extract the waste for a second time. Pulp and olive stone are the constituents of the raw material mixture, with a particle size between 0.2 and 9 mm. Firstly; proximate analysis was conducted to characterize the olive waste samples. Olive waste samples were oven dried for almost an hour at  $105^{\circ}\text{C}$ . Drying was performed to ensure that samples are dry and ready for grinding and screening. Afterwards, these samples were grinded in a pin type mill to reduce their particle size. After that, the samples were screened for different particle sizes employing a Vibro sieving machine. The proximate analysis was performed following the procedure given by Miranda et al. [30]. The following results were obtained: moisture content 8%, volatile

matter 43%, fixed carbon 45%, and ash 4%. Calorific value of olive waste was obtained using a standard bomb calorimeter. Secondly; a thermolyne silica electric oven was used to carry out the activation processes with a temperature control device linked to a thermocouple, a silicon reactor, and a steam generator. The activation periods were in the range of 30–80 min and the activation temperatures were between 1022 and 1122 K. Detailed procedure for olive waste activation is given in Bacfaoui et al. [31]. Following activation, the activated product was boiled for 30 min in distilled water, dried, and crushed. The activated olive waste was then dried at 380 K until unvarying weight reached and then reserved in a sealed tight container for upcoming use.

### 3.2. Experimental method

A vacuum pump was used at the beginning to prove the system for any leakage and to suck out entrapped air or moisture. The system was evacuated at elevated temperature until a pressure of –22 kPa was obtained in the system. Accordingly, the system was left for a while and all founded leaks were quickly sealed. After that, the system was washed by liquid methanol for about 30 min. Then, the adsorbent was charged with methanol. The charging process continued over night so that the greatest quantity of adsorbate achievable could be sorbed prior to the solar heating process the day after. Solar heating started in the morning, with the adsorber at surrounding temperature and the highest achievable concentration of adsorbate adsorbed on the activated carbon particles and with all valves closed. While the solar heating proceeded, the pressure in the system increased with the adsorbed methanol mass continued to be fixed. When the desorption of methanol started, indicated by a reading of gauge pressure of about 13 kPa inside the tubes in the bed, two valves were opened; the one linking the bed tubes and the condenser and the one linking the condenser with the receiver, while the other valves kept closed. The desorbed methanol vapor left the bed tubes was changed into liquid methanol in the condenser. All necessary data; bed temperature, tube surface temperature, ambient temperature, condenser temperature, refrigerated space temperature, and bed pressure were observed and registered during this process. Generally, the highest cycle temperature was attained at around 13:30. The process of methanol generation and condensation continued until no perceptible change in the condensate level was noticed. This point was constantly reached at about 3 h after reaching the highest temperature in the cycle. The temperature and pressure of the system dropped quickly at sunset. As cooling proceeded, the valve linking the liquid receiver with the evaporator was opened to allow the condensate into the evaporator coil. Afterward, the previous valve was closed, while the valve connecting the adsorber with the evaporator was opened to allow the evaporated methanol vapor re-sorption.

### 4. Estimation of the performance

The COP is the capacity of cooling attained by a refrigeration device per unit of heat provided. The  $COP_{ref}$  of a sorption refrigerator operating is calculated by the second law of thermodynamics. Detailed derivation of  $COP_{ref}$  is given in [32]. The derivation led to Eq. (1) below:

$$COP_{ref} = T_e(T_g - T_a)/T_g(T_a - T_c) \quad (1)$$

where  $T_g$  is the generating temperature,  $T_a$  is ambient temperature,  $T_e$  is evaporating temperature, and  $T_c$  is condensing temperature. However, Critoph [33] established another expression for ideal adsorption refrigerators  $COP_{ref(ad)}$

$$COP_{ref(ad)} = T_e/T_{ad} = T_e/T_g \quad (2)$$

where  $T_{ad}$  is the average adsorption temperature.

The parameters used in producing the experimental outcomes are defined as follows:  $Q_{it}$  is the total incident global solar energy and is calculated by multiplying  $G_i$  (the incident global solar flux during the entire day) and  $A_e$  (the exposed surface area of the collector):

$$Q_{it} = G_i A_e \quad (3)$$

$Q_{ic}$  is the transmitted useful heat energy to the adsorbent to drive out methanol and is calculated by adding the latent heat of generation of methanol ( $m_r h_{sg}$ ) to the sensible heat absorbed by the adsorbent and methanol ( $m_{ow} h_{ow} + m_r C_p \Delta T_g$ ) as given by [20]:

$$Q_{ic} = m_{ow} h_{ow} + m_r C_p \Delta T_g + m_r h_{sg} \quad (4)$$

where  $m_{ow}$  and  $m_r$  are the mass of olive waste and mass of methanol in kg, respectively;  $C_p$  is specific heat capacity of olive waste and methanol in kJ/kg °C, respectively;  $h_{ow}$  is calorific value of olive waste in kJ/kg; and  $h_{sg}$  is the enthalpy of solid–gas phase of methanol in kJ/kg.

As given by [20], the useful cooling produced ( $Q_{uc}$ ) in case of ice-producing cycle can be calculated by knowing the amount of water ( $m_w$ ) brought in thermal contact with the evaporator compartment and undergoes a temperature change of  $\Delta T_w$  to generate quantity of ice ( $m_i$ ):

$$Q_{uc} = m_w C_{p_w} \Delta T_w + m_i C_{p_i} \Delta T_i + m_i h_{sf} \quad (5)$$

where  $C_{p_w}$  and  $C_{p_i}$  are specific heat capacity of water and ice in kJ/kg °C, respectively, and  $h_{sf}$  is the enthalpy of solid–liquid phase of ice in kJ/kg.

The available or gross heat extraction ( $Q_a$ ) is given by:

$$Q_a = m_r h_{fg} \quad (6)$$

where  $h_{fg}$  is the liquid–gas phase enthalpy of methanol in kJ/kg.

This is also the capacity of condensate cooling. From the preceding information, the performance indicators of the solar refrigerator system are evaluated as follows [20]:

$COP_a$ , is the available or gross cycle coefficient of performance and is given by:

$$COP_a = Q_a/Q_{ic} \quad (7)$$

$COP_{uc}$ , is the useful or actual cycle coefficient of performance and is given by:

$$COP_{uc} = Q_{uc}/Q_{ic} \quad (8)$$

$COP_{ao}$  is the available gross or over all coefficient of performance and is given by:

$$COP_{ao} = Q_a/Q_{it} \quad (9)$$

$COP_{uo}$  is the useful or actual overall coefficient of performance and is given by:

$$COP_{uo} = Q_{uc}/Q_{it} \quad (10)$$

The efficiency ( $\eta$ ) of solar collector/adsorber is given by:

$$\eta = Q_{ic}/Q_{it} \quad (11)$$

From the results obtained, the highest  $COP_a$  obtained was 0.75. Multiple regressions were utilized to arrive at the parameters of the optimum region of the solar adsorption system using Minitab [34].

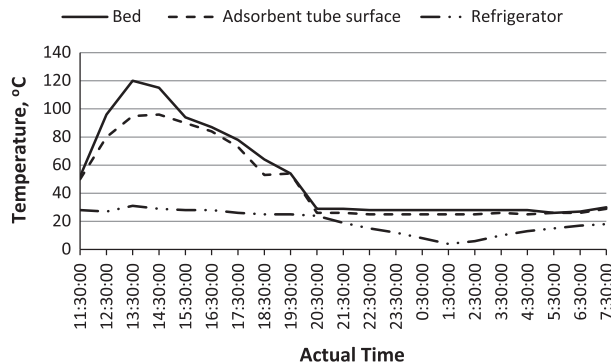
### 5. Results and discussion

Table 2 shows an example of the actual the data used to determine the  $\eta$  and the COP of the entire device. Fig. 2 shows an example of the data harvest output for 1 day. It presents the temperature variations of the bed, refrigerator, and the adsorbent



**Table 2**General data used to calculate  $COP$  and  $\eta$  for the whole unit.

|  |                         |
|--|-------------------------|
| Global solar radiation on site, $G_i$              | 0.650 kW/m <sup>2</sup> |
| Adsorbent/adsorbate pair                           | Olive waste/methanol    |
| Average ambient temperature, $T_a$                 | 25 °C                   |
| Maximum generation temperature, $T_g$              | 120 °C                  |
| Condensing temperature, $T_c$                      | 25 °C                   |
| Evaporating temperature, $T_e$                     | 8 °C                    |
| Specific heat capacity of methanol, $C_{p_r}$      | 22.545 kJ/kg °C         |
| Olive waste calorific value, $h_{ow}$              | 32.460 kJ/kg            |
| Enthalpy of solid–gas phase of methanol, $h_{sg}$  | 1400 kJ/kg              |
| Enthalpy of liquid–gas phase of methanol, $h_{lg}$ | 1100 kJ/kg              |

**Fig. 2.** Variations of bed, refrigerator, and adsorbent tube surface temperatures with time.

tube surface with actual time when each measurement was taken. The effective refrigeration started at 20:30 which is the time the heat started to diminish steadily till the temperature reached 4 °C at 01:30 the other day then it increased again. Generally, the changes in bed temperature were almost in accordance with the changes in the temperature of the adsorbent tube surface. A sharp increase in the adsorbent tube surface temperatures took place constantly between 9:30 and 12:30 prior to the beginning of methanol condensation. At this phase, the temperature and pressure of the system were increased. This is indicated by the knee on the curve of the adsorbent tube surface temperature, which is visible at around 3 h from the start of heating. Condensation started at pressure of about 13 kPa. The desorbed methanol was cooled in the condenser and liquid methanol accumulated in the liquid receiver. Throughout the processes of methanol desorption and condensation, the unit pressure increased at a slower rate compared to its rate of increase prior to the start of condensation. That is because the bleeding of some methanol decreased the rate of forming of methanol gas inside the system and, as a result, decreased the rate of increase of the pressure in the unit even though the solar heating still continued; the pressure would not increase as fast as before. In general, the adsorbent tube surface temperature attained about 95 °C and stayed above 70 °C over 5 h of heating interval. The highest temperature reached by the collector was 120 °C. After the climax, the bed temperature, the system pressure, and the adsorbent tube surface temperature decreased with the waning of solar energy amount. From the cooling curve of Fig. 2, it can be noticed that the adsorbent tube surface temperature decreased to a lowest value at about 3 h after cooling started and increased slightly another time before attaining a different minimum value. This tendency is to be anticipated because the start of significant adsorption and the accompanying rejection of heat slowed the cooling of the adsorbent. The lowest cooling temperature achieved in this unit varied in the range of 4.0–7.5 °C for water that already started the cooling process with temperature in the range of 23–26 °C.

The system performance as evaluated using the data harvest output for the day shown in Fig. 2 is as follow:  $COP_a = 0.76$ ,  $COP_{uc} = 0.097$ , and  $COP_{uo} = 0.026$ . The efficiency of the collector attained in this study was 19.3%. Overall, the new design of the adsorption system did improve the performance over the earlier system presented in Abu-Hamdeh and Al-Muhtaseb [2].

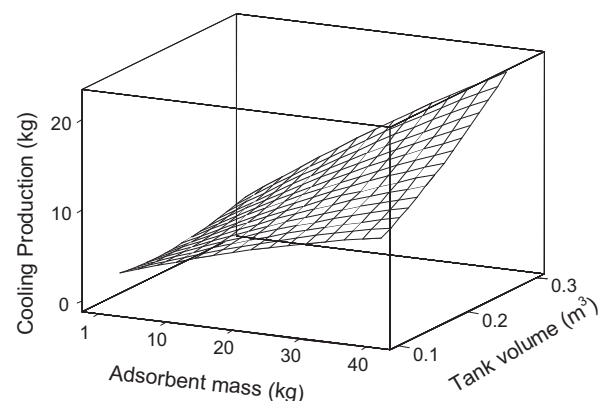
Multiple regression technique was used to analyze data and arrive to the optimum region of the solar adsorption system parameters. Minitab [34], a statistical package, was used for response surface analysis and optimization. The two variables model for a response surface design is:

$$Y = \beta_0 + \beta_1 x_1 + \beta_2 x_2 + \beta_{11} x_1^2 + \beta_{22} x_2^2 + \beta_{12} x_1 x_2 + \varepsilon \quad (12)$$

where  $Y$  is the dependent variable or response;  $\beta_0$  is constant term;  $\beta_i$  is regression coefficients which indicate the importance of their associated  $x$  value;  $x_i$  is regressor variables or independent variables in the solar adsorption system;  $\varepsilon$  is the random error term.

$Y$  (the dependent variable) is a function of  $x_1$ ,  $x_2$  (the independent variables) and  $\varepsilon$  (the experimental error term). The error term is a statistical error that is presumed to have normal distribution with zero mean and variance  $\sigma^2$ .

Response surface plot is a three-dimensional graph that shows the response surface from the side in which each value of the independent variables,  $x_1$  and  $x_2$ , generates a  $Y$ -value. Fig. 3 shows the response surface of the cooling production of the refrigerator as a function of adsorbent mass and tank volume. The optimal value of the cooling production located in the zone where the adsorbent mass ranged from 30 to 40 kg and tank volume lies between 0.2 and 0.3 m<sup>3</sup>. It is observed that the cooling production increased when the mass increased providing the adsorbent mass is less than 40 kg. The increase in adsorbent mass implies extra methanol being adsorbed at the beginning of the cooling process. Thus, additional vapor of methanol can be desorbed during desorption phase, which yields further cooling. Nevertheless, if the mass of the adsorbent is increased to more than 40 kg, the cooling production reduced. This occurred for the reason that with the existing heat input, just the bed could be heated, and this is not enough to desorb the necessary amount of methanol. Fig. 4 discusses the adequacy of the response surface of cooling production as a function of tank volume and adsorbent mass. Analysis of Variance (ANOVA) of the data was used to confirm the adequacy of the model at  $p < 0.10$ . A hypothesis that the error term  $\varepsilon$  in the regression model is normally and independently distributed with mean zero and  $\sigma^2$  was tested. The results failed to reject the hypothesis. As shown in Fig. 4, the residuals are ordinarily and separately distributed with no crystals or cretin distributed shape, The  $R^2$  and adjusted  $R^2$  val-

**Fig. 3.** The system response surface of the cooling production as a function of tank volume and adsorbent mass.

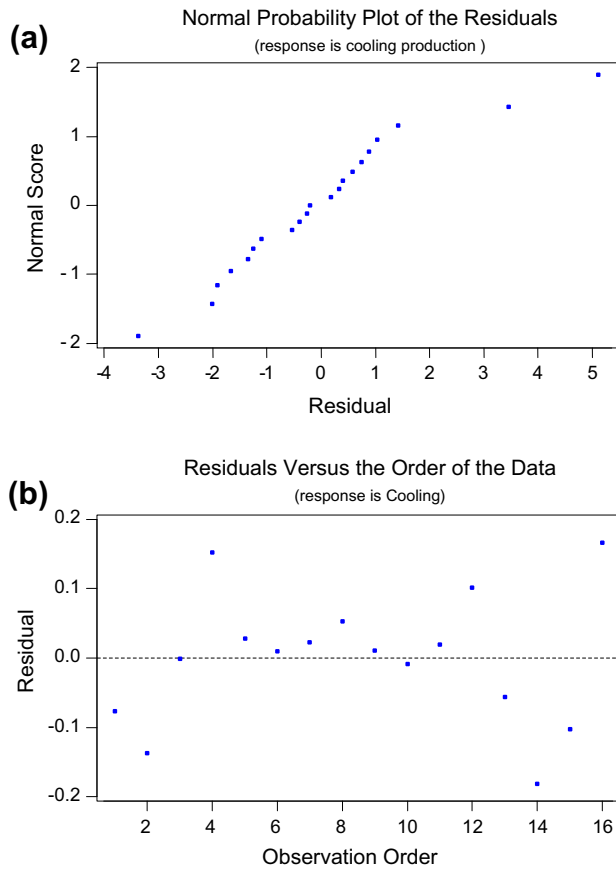


**Fig. 4.** (a) Normal probability plot of the residuals of cooling production as a function of tank volume and adsorbent mass, and (b) residuals versus the order of the data of the response of cooling production.

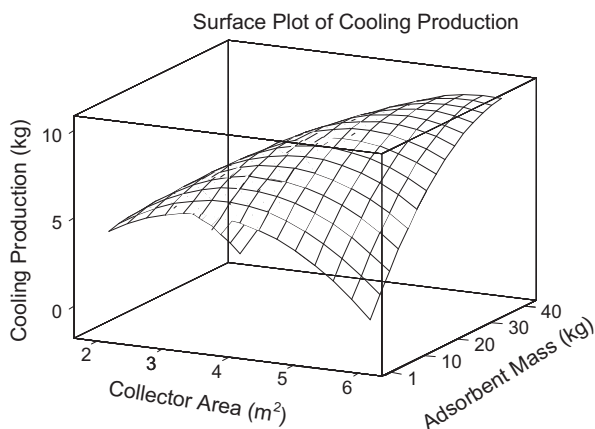


**Fig. 5.** Response surface of the cooling production of the system as a function of adsorbent mass and collector area.

ues were estimated as 99.5% and 99.4%, respectively, an indication that the model has a good fit.

Fig. 5 illustrates the response surface of the cooling production of the refrigerator as a function of collector area and adsorbent mass. The best possible value of the cooling production located in the zone where the adsorbent mass is from 30 to 40 kg, and collector area between 3.5 and 5 m<sup>2</sup>. Again, the cooling production increased given that the mass of the adsorbent stays below than 40 kg and it decreased if the adsorbent mass becomes above

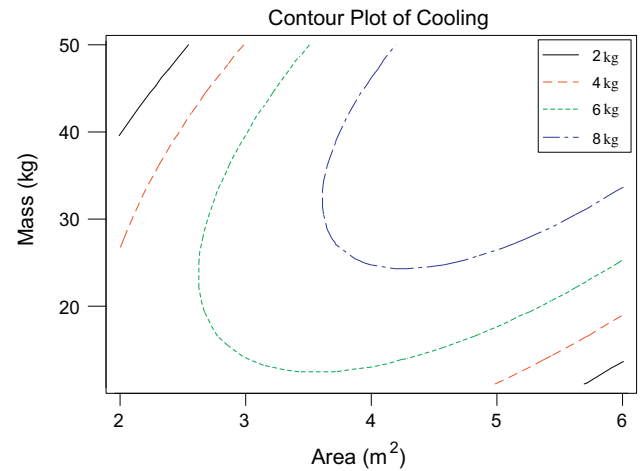


**Fig. 6.** Contour plot of the cooling production of the system as a function of adsorbent mass and collector area.

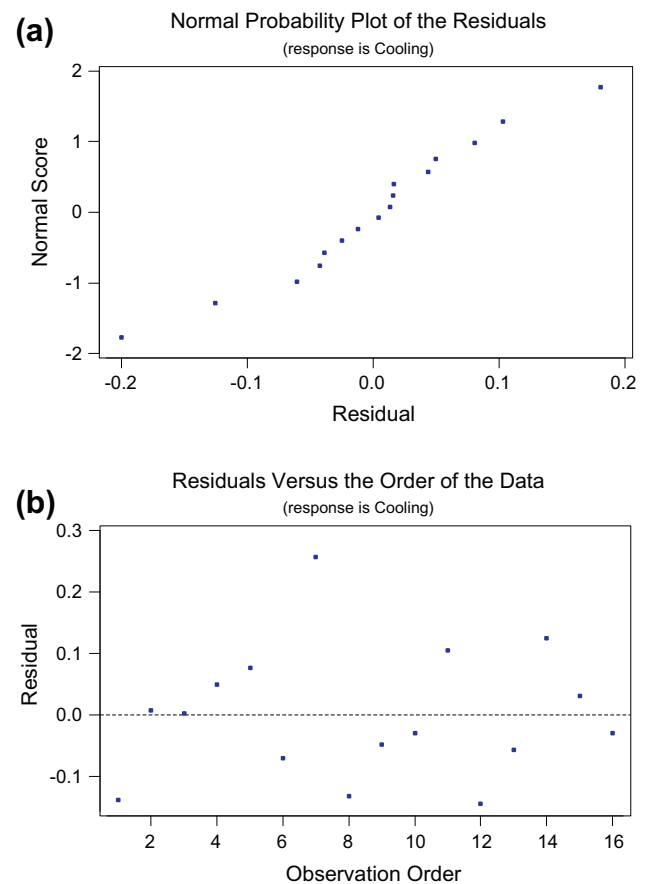


**Fig. 7.** (a) Normal probability plot of the residuals of the response of cooling production as a function of adsorbent mass and collector area, and (b) residuals versus the order of the data of the response of cooling production.

40 kg for the same reason given earlier. Occasionally, it is easier to show two-dimensional graphs, called contour plots, for the response surface. The main feature of the contour plots that they can present contour lines of the independent variables pair ( $x_1$  and  $x_2$ ) that have equal response value  $Y$ . Fig. 6 illustrates the cooling production in terms of contour plot as a function of collector area and adsorbent mass. The figure presents once more that the

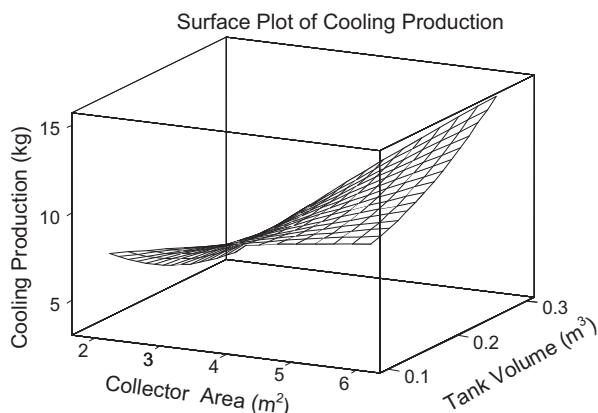


Fig. 8. Response surface of the cooling production of the system as a function of tank collector area and volume.

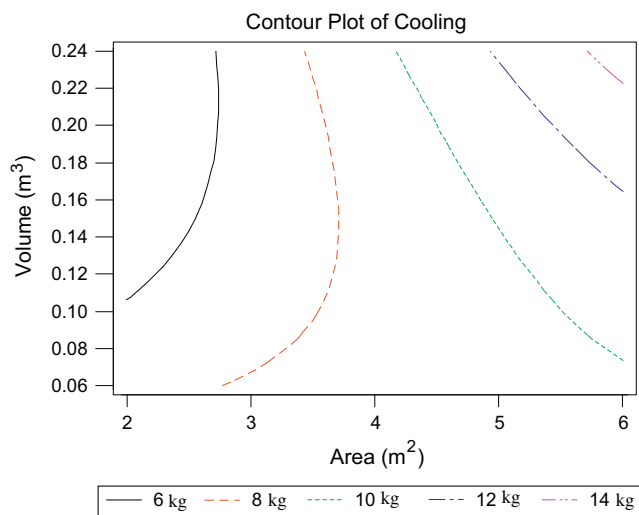


Fig. 9. The system contour plot of the cooling production as a function of tank volume and collector area.

optimum domain of cooling production is when the mass of the adsorbent lies between 30 and 40 kg and when the collector area lies between 3.5 and 5 m<sup>2</sup>. Fig. 7 discusses the adequacy of cooling production response surface plot as a function of adsorbent mass and collector area. The same hypothesis for the error term  $\varepsilon$  was tested again as before. Again, independent and normal distribution of the residuals are shown in the figure with no crystals or cretin distributed shape. The values of  $R^2$  and adjusted  $R^2$  were calculated to be 99.5% and 99.3%, respectively, which indicate a good fit of the model. The combined effect of the process variables is significant at  $p < 0.10$ .

Fig. 8 shows the response surface of the cooling production of the unit as a function collector area and tank volume. As the figure presents, the best possible value of the cooling production was found in the zone where the tank volume lies between 0.2 and 0.3 m<sup>3</sup>, and collector area lies between 3.5 and 5 m<sup>2</sup>. Fig. 9 shows the cooling production in terms of contour plot for the solar unit as a function of collector area and tank volume. The figure illustrates once again that the most favorable region of cooling production is when the tank volume lies between 0.2 and 0.3 m<sup>3</sup>, and when the collector area lies between 3.5 and 5 m<sup>2</sup>. Fig. 10 discusses the response surface adequacy of cooling production as a function of collector area and tank volume. As shown, the distribution of the residuals is normal and independent with no crystals or cretin dis-

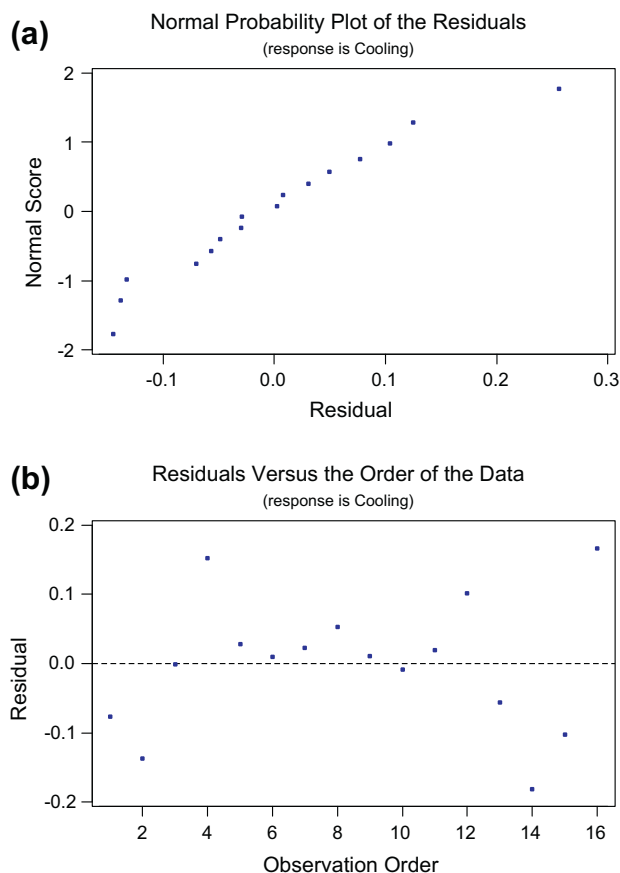


Fig. 10. (a) Normal probability plot of the residuals of the response of cooling production as a function of tank volume and collector area, and (b) residuals versus the order of the data of the response of cooling production.

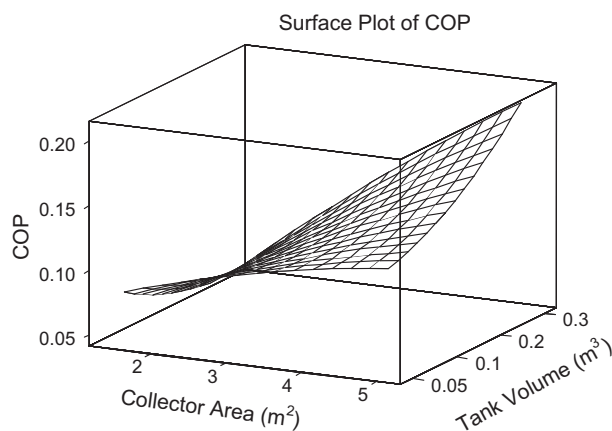


Fig. 11. Response surface of the COP of the system as a function of tank volume and collector area.

tributed shape. The calculated  $R^2$  and adjusted  $R^2$  values were 99.8% and 99.7%, respectively.

Fig. 11 shows the COP response surface as a function of tank volume and collector area. It implies that the best value of COP located in the zone where the collector area ranged from 3.5 to 5 m<sup>2</sup>, and tank volume ranged from 0.2 to 0.3 m<sup>3</sup>. The water could attain the required desorption temperature much earlier in case of low tank volumes which, in turn, influences the performance of the system. A collector area beyond 5 m<sup>2</sup> reduced the COP of the system. This is because the cooling production does not boost much after the

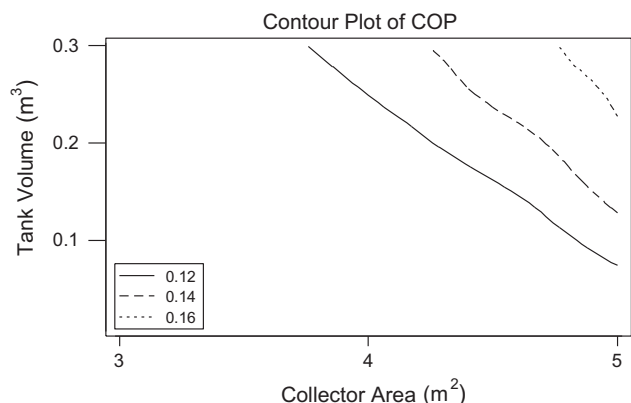


Fig. 12. Contour plot of the COP of the system as a function of tank volume and collector area.

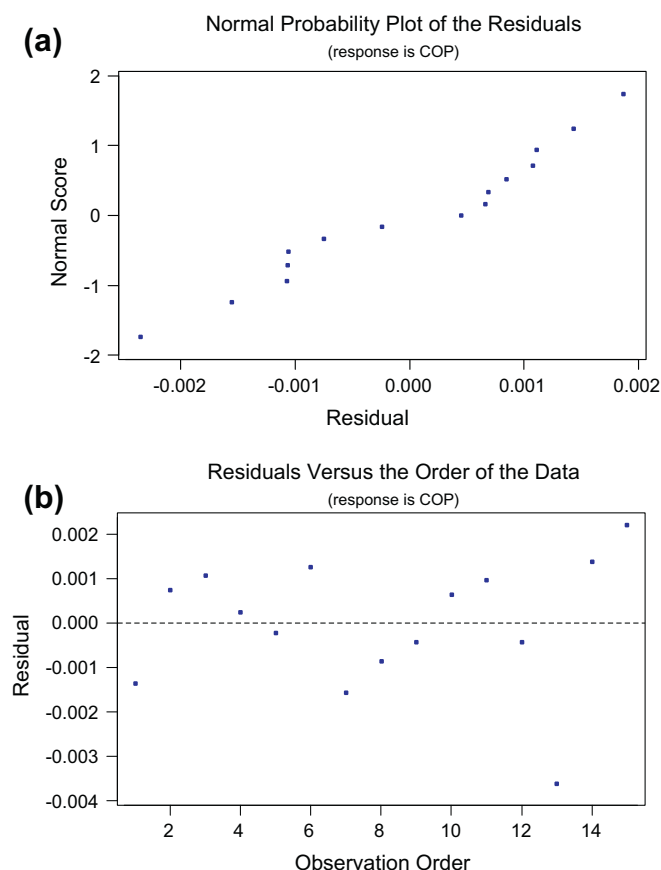


Fig. 13. (a) Residuals versus the order of the data of the response of COP, and (b) normal probability plot of the residuals of the response of COP as a function tank volume and collector area.

water temperature becomes beyond 100 °C, which is the expected temperature for water to reach if the collector area is beyond 5 m<sup>2</sup>. Thus, with additional increase of heat in the water, which is a consequence of the increasing collector area, the cooling production remained constant, but the COP decreased. The contour plot of the system COP as a function of tank volume and collector area is shown in Fig. 12. Once again, the optimum value of the COP lies in the zone where the collector area is given from 3.5 to 5 m<sup>2</sup>, and tank volume ranged from 0.2 to 0.3 m<sup>3</sup>. Fig. 13 discusses the competence of the response surface of the COP as a function of tank

volume and collector area. As before, the residuals are normally and independently distributed with no crystals or cretin distributed shape. The calculated values of  $R^2$  and adjusted  $R^2$  were 99.4% and 99.3%, respectively.

## 6. Conclusions

An improved prototype of an adsorption cooling system with particular specifications and requirements was investigated in this paper. The suggested device is powered by a parabolic trough solar collector (PTC) and uses olive waste (as an adsorbent) with methanol (as an adsorbate) forming an adsorbent–adsorbate pair. The archetype has been verified by using experimental results and statistical method. The least possible temperature reading acquired for the refrigerator was 4 °C while the calculated gross cycle coefficient of performance,  $COP_g = 0.75$ . It has been demonstrated that expanding the adsorbent mass to a certain range increases the coefficient of performance. The results obtained from statistical technique showed that the optimal adsorbent mass varied between 30 and 40 kg. Furthermore, increasing the tank volume to particular limits increased the coefficient of performance. The results obtained from statistical optimization revealed that the optimum tank volume varied between 0.2 and 0.3 m<sup>3</sup>. In addition, increasing the collector area to a certain range increased the coefficient of performance. The results obtained from applying the statistical techniques showed also that the optimum collector area varied between 3.5 and 5 m<sup>2</sup>. The statistical value of the solar coefficients of performance of the system varied from 0.18 to 0.2. The results demonstrate the successes of using olive waste/methanol as an adsorbent/adsorbate pair in solar refrigeration applications. Olive waste satisfies the most important requirements that affect the selection process of an appropriate adsorbent; adsorption of considerable quantity of the adsorbate in low temperature states to produce acceptable COP; desorption of most of the adsorbate when exposed to thermal energy; non-corrosive and non-toxic; low-cost and generally available in most developing countries.

## References

- [1] Anyanwu EE. Review of solid adsorption solar refrigerator I: an overview of the refrigeration cycle. *Energy Convers Manage* 2003;44:301–12.
- [2] Abu Hamdeh NH, Al-Muhtaseb MA. Optimization of solar adsorption refrigeration system using experimental and statistical techniques. *Energy Convers Manage* 2010;51:1610–5.
- [3] Hassan HZ, Mohamad AA. A review on solar cold production through absorption technology. *Renew Sust Energy Rev* 2012;16:5331–48.
- [4] Gonzalez MI, Rodriguez LR. Solar powered adsorption refrigerator with CPC collection system. *Energy Convers Manage* 2007;48:2587–94.
- [5] Hassan HZ, Mohamad AA, Al-Ansary HA. Development of a continuously operating solar-driven adsorption cooling system: thermodynamic analysis and parametric study. *Appl Therm Eng* 2012;48:332–41.
- [6] Hassan HZ, Mohamad AA. A review on solar-powered closed physisorption cooling systems. *Renew Sust Energy Rev* 2012;16:2516–38.
- [7] Choudhury B, Saha BB, Chatterjee PK, Sarkar JP. An overview of developments in adsorption refrigeration systems towards a sustainable way of cooling. *Appl Energy* 2013;104:554–67.
- [8] El Fadar A, Mimet A, Pérez-García M. Modelling and performance study of a continuous adsorption refrigeration system driven by parabolic trough solar collector. *Sol Energy* 2009;83:850–61.
- [9] Habib K, Saha BB, Chakraborty A, Koyama S, Srinivasan K. Performance evaluation of combined adsorption refrigeration cycles. *Int J Refrig* 2011;34:129–37.
- [10] Hassan HZ, Mohamad AA, Bennacer R. Simulation of an adsorption solar cooling system. *Energy* 2011;36:530–7.
- [11] Kalogirou S, Lloyd S. Use of solar parabolic trough collectors for hot water production in Cyprus. A feasibility study. *Renew Energy* 1992;2:117–24.
- [12] Kalogirou S. Parabolic trough collector system for low temperature steam generation: design and performance characteristics. *Appl Energy* 1996;55:1–19.
- [13] Kalogirou S. Use of parabolic trough solar energy collectors for sea-water desalination. *Appl Energy* 1998;60:65–88.
- [14] Zarza E, Valenzuela L, León J, Hennecke K, Eck M, Eck M, et al. Direct steam generation in parabolic troughs: final results and conclusions of the DISS project. *Energy* 2004;29:635–44.



- [15] Alam KCA, Khan MZI, Uyun AS, Hamamoto Y, Akisawa A, Kashiwagi T. Experimental study of a low temperature heat driven reheat two-stage adsorption chiller. *Appl Therm Eng* 2007;27:1686–92.
- [16] Valan Arasu A, Sornakumar T. Design, manufacture and testing of fiberglass reinforced parabola trough for parabolic trough solar collectors. *Sol Energy* 2007;81:1273–9.
- [17] Badran O, Eck M. The application of parabolic trough technology under Jordanian climate. *Renew Energy* 2006;31:791–802.
- [18] Valan Arasu A, Sornakumar T. Performance characteristics of parabolic trough solar collector system for hot water generation. *Int Energy J* 2006;7:137–45.
- [19] Anyanwu EE. Review of solid adsorption solar refrigeration II: an overview of the principles and theory. *Energy Convers Manage* 2004;45:1279–95.
- [20] Anyanwu EE, Ezekwe CI. Design, construction and test run of a solid adsorption solar refrigerator using activated carbon/methanol, as adsorbent/adsorbate pair. *Energy Convers Manage* 2003;44:2879–92.
- [21] Leite APF, Daguenet M. Performance of a new solid adsorption ice maker with solar energy regeneration. *Energy Convers Manage* 2000;41:1625–47.
- [22] Ng KC. Recent developments in heat-driven silica gel–water adsorption chillers. *Heat Transfer Eng* 2003;24:1–3.
- [23] Wang DC, Shi ZX, Yang QR, Tian XL, Zhang JC, Wu JY. Experimental research on novel adsorption chiller driven by low grade heat source. *Energy Convers Manage* 2007;48:2375–81.
- [24] Chakraborty A, Saha BB, Koyama S, Ng KC, Srinivasan K. Adsorption thermodynamics of silica gel–water systems. *J Chem Eng Data* 2009;54:448–52.
- [25] Critoph RE, Vogel R. Possible adsorption pairs for use in solar cooling. *Int J Ambient Energy* 1986;7:183–90.
- [26] Karaca S, Gürses A, Bayrak R. Investigation of applicability of the various adsorption models of methylene blue adsorption onto lignite/water interface. *Energy Convers Manage* 2005;46:33–46.
- [27] El-Sharkawy II, Hassan M, Saha BB, Koyama S, Nasr MM. Study of adsorption of methanol onto carbon based adsorbents. *Int J Refrig* 2009;34(32):1579–86.
- [28] Chakraborty A, Saha BB, Ng KC, Koyama S, Srinivasan K. Theoretical insight of physical adsorption for a single component adsorbent + adsorbate system: II. The Henry region. *Langmuir* 2009;25:7359–67.
- [29] Fernando A, Monteiro S, Pinto F, Mendes B. Production of biosorbents from waste olive cake and its adsorption characteristics for  $Zn^{2+}$  ion. *Sustainability* 2009;1:277–97.
- [30] Miranda T, Esteban A, Rojas S, Montero I, Ruiz A. Combustion analysis of different olive residues. *Int J Mol Sci* 2008;9:512–25.
- [31] Bacfaoui A, Yaacoubi A, Dahbi A, Bennouna C, Phan Tan Luu R, Maldonado-Hodar FJ, et al. Optimization of conditions for the preparation of activated carbons from olive-waste cakes. *Carbon* 2001;39:425–32.
- [32] Al-Muhtaseb M. Design of solar adsorption refrigeration unit, Master Thesis in Mechanical Engineering Department, Jordan University of Science and Technology, Jordan; 2008.
- [33] Critoph RE. Performance limitations of adsorption cycles for solar cooling. *Sol Energy* 1988;41:21–31.
- [34] MINITAB., Minitab Release 10.2. Minitab Inc. State College, PA; 1994.